Resonant inelastic x-ray scattering spectra in the hyperhoneycomb iridate β-Li_2IrO_3: First-principles calculations

V. N. Antonov,[1,2] D. A. Kukusta,[1,3] L. Uba,[2] A. Bonda,[2] and S. Uba[2]

[1]*G. V. Kurdyumov Institute for Metal Physics, NAS of Ukraine, 36 Academician Vernadsky Boulevard, UA-03142 Kyiv, Ukraine*

[2]*Faculty of Physics, University of Bialystok, K. Ciolkowskiego 1L, PL-15-245 Bialystok, Poland*

[3]*Max-Planck-Institut für Festkörperforschung, Heisenberg Strasse 1, D-70569 Stuttgart, Germany*

(Received 1 February 2021; revised 26 April 2021; accepted 3 June 2021; published 14 June 2021)

We studied the electronic structure of the β-Li_2IrO_3 insulator within the density-functional theory using the generalized gradient approximation while taking into account strong Coulomb correlations in the framework of the fully relativistic spin-polarized Dirac linear muffin-tin orbital band structure method. The β-Li_2IrO_3 undergoes a pressure-induced structural and magnetic phase transition at $P_c \sim 4$ GPa with symmetry lowering to the monoclinic $C2/c$. The structural phase transition is accompanied by the formation of Ir_2 dimers on the zigzag chains, with an Ir-Ir distance of ~2.66 Å, even shorter than that of metallic Ir. The strong dimerization stabilizes the bonding molecular-orbital state, leads to the collapse of the magnetism, and opens the energy gap with a concomitant electronic phase transition from a Mott insulator to band insulator. The resonant inelastic x-ray scattering spectra (RIXS) at the Ir L_3 edge were investigated theoretically from first principles. The calculated results are in good agreement with the experimental data. We show that the drastic reconstruction of the RIXS spectral peak at 0.7 eV associated with the structural $Fddd \rightarrow C2/c$ phase transition at P_c can be related to the disappearing of the Coulomb correlations in the high-pressure $C2/c$ phase.

DOI: 10.1103/PhysRevB.103.235127

I. INTRODUCTION

Quantum spin liquids (QSLs) [1–3] represent a novel state of matter in which quantum fluctuations prevent the conventional magnetic order from being established, and the spins remain disordered even at zero temperature. It is an emerging and fast growing field. In this context the Kitaev Hamiltonian on honeycomb lattices has great promise [4]. The paramount attention given to such states can be understood by the fact that they may be topologically protected from decoherence [5], display fractional excitations with Majorana statistics, and therefore hold promise in the field of quantum information and quantum computation [6,7]. The field of QSLs is still wide open, both theoretically and experimentally. So far, there have been new experimental discoveries, and theoretical ideas are rapidly emerging. However, a basic mathematical framework that can be used to understand QSLs systematically is still lacking. The major difficulty in understanding QSLs is that they are intrinsically strongly correlated systems, for which no perturbative approach is available.

Possible realization of such an exotic state has been suggested in Mott insulators such as the 213 iridates A_2IrO_3 (with A = Na, Li), which have a honeycomb layered structure consisting of IrO_6 octahedra [6,8]. They have drawn much attention as a candidate for topological insulators [9,10] with electron correlations. Both nontrivial hopping terms induced by the strong spin-orbit (SO) coupling and significant on-site Coulomb correlations make honeycomb iridates a possible candidate also for the compounds with a Kitaev spin liquid type ground state [11–17]. It was proposed that strong SO interaction in these iridates reorganizes the crystal field states of the $5d$ orbitals into a J-multiplet structure, where J is the combined spin and effective orbital angular momentum. In this case, the Ir t_{2g} bands are most naturally described by relativistic atomic orbitals with the effective total angular momentum, $J_{\text{eff}} = 3/2$ and $J_{\text{eff}} = 1/2$. In this approximation, the splitting between the $3/2$ and $1/2$ states is larger than their dispersion. The $J_{\text{eff}} = 1/2$ band is half filled, and the relatively weak Coulomb repulsion U is sufficient to split the $J_{\text{eff}} = 1/2$ doublet into lower and upper Hubbard bands, giving rise to a novel Mott insulator [18].

There are several recent publications on the experimental and theoretical investigations of the electronic structure and various physical properties of honeycomb iridate Li_2IrO_3 [13,19–28]. However, the long-sought spin-liquid state has remained elusive. All three honeycomb polytypes of Li_2IrO_3 (including the α, β, and γ phases) are magnetically ordered, which suggests that the Heisenberg interaction is still sizable. In addition, trigonal crystal fields also compete with the Kitaev interaction.

In the present study, we focus our attention on the theoretical investigation of the resonant inelastic x-ray scattering (RIXS) spectra in the β-Li_2IrO_3 compound from first principles. RIXS is a fast developing experimental technique in which one scatters x-ray photons inelastically off matter. It is a photon-in, photon-out spectroscopy for which one can, in principle, measure the energy, momentum, and polarization change of the scattered photon. Compared to other scattering techniques, RIXS has number of unique features. It covers a large scattering phase space and is polarization dependent,

element and orbital specific, and bulk sensitive [29]. The RIXS spectra at the Ir $L3$ edge in β-Li_2IrO_3 were measured by Takayama *et al.* [27] as a function of applied hydrostatic pressure. β-Li_2IrO_3 undergoes a pressure-induced structural phase transition at $P_c \sim 4$ GPa with symmetry lowering to the monoclinic $C2/c$. The structural phase transition is accompanied by the formation of Ir_2 dimers on the zigzag chains, with an Ir-Ir distance of ∼2.66 Å, even shorter than that of metallic Ir. The strong dimerization stabilizes the bonding molecular-orbital state, leads to the collapse of the magnetism, and opens the energy gap with a concomitant electronic phase transition from a Mott insulator to a band insulator [27]. The experimental measurements showed the drastic reconstruction of the RIXS spectra associated with this dimerization [27]. With increasing pressure above P_c the prominent peak at ∼0.7 eV is suppressed strongly. The one at 3.5 eV is broadened but remains in the high-pressure phase. There are some changes in the 0.5 to 2.0 eV energy interval, and a shoulderlike feature around 2.8 eV emerges. The aim of the present work is to investigate the RIXS spectra in the β-Li_2IrO_3 compound from first principles and its evolution under pressure-induced structural phase transitions.

This paper is organized as follows. The computational details are presented in Sec. II. Section III presents the electronic structure and theoretically calculated RIXS spectra of the β-Li_2IrO_3 compound compared with the experimental measurements. Finally, the results are summarized in Sec. IV.

II. COMPUTATIONAL DETAILS

a. Crystal structure. β-Li_2IrO_3 crystallizes in the orthorhombic space group $Fddd$, with zigzag chains running in alternating directions (see Fig. 1 in Ref. [30] and Fig. 1 in Ref. [27]). In the language of the Kitaev interactions, these chains form the x and y bonds, while the z bonds link together adjacent layers of chains. In the hyperhoneycomb Ir sublattice of β-Li_2IrO_3, the zigzag Ir chains are connected by the bridging bonds parallel to the c axis; all the angles between the three Ir-Ir bonds are close to 120°, and the distances between Ir atoms are almost equal (only ∼0.2% difference). At ambient pressure, Ir-Ir bonds along zigzag chains have a length $d_{x,y} = 2.9729$ Å, and bonds between the chains $d_z = 2.9784$ Å.

As pressure increases from ambient pressure to 3.08 GPa, the $d_{x,y}$ Ir-Ir bonds shrink from 2.9729 to 2.9246 Å; the corresponding d_z Ir-Ir bonds also decrease from 2.9784 to 2.9379 Å [27,31]. At P_c, the bonds between the chains d_z slightly increase to 3.0129 Å; one of the x/y bonds also increases to 3.0143 Å, while the other one decreases strongly to 2.6609 Å. Note that this distance is even smaller than the Ir-Ir distance of 2.714 Å in Ir metal. Such a remarkably small interatomic distance strongly suggests the formation of Ir_2 dimers at P_c [27]. The pressure dependence of the structural parameters of the orthorhombic β-Li_2IrO_3 can be found in Refs. [27,31].

b. Resonant inelastic x-ray scattering. In the direct RIXS process [29] an incoming photon with energy $\hbar\omega_{\mathbf{k}}$, momentum $\hbar\mathbf{k}$, and polarization $\boldsymbol{\epsilon}$ excites the solid from a ground state $|\mathrm{g}\rangle$ with energy E_g to the intermediate state $|\mathrm{I}\rangle$ with energy E_I. During relaxation an outgoing photon with energy $\hbar\omega_{\mathbf{k}'}$, momentum $\hbar\mathbf{k}'$, and polarization $\boldsymbol{\epsilon}'$ is emitted, and the solid is in state $|f\rangle$ with energy E_f. As a result an excitation with energy $\hbar\omega = \hbar\omega_{\mathbf{k}} - \hbar\omega_{\mathbf{k}'}$ and momentum $\hbar\mathbf{q} = \hbar\mathbf{k} - \hbar\mathbf{k}'$ is created. Our implementation of the code for the calculation of the RIXS intensity uses Dirac four-component basis functions [32] in the perturbative approach [33]. RIXS is the second-order process, and its intensity is given by

$$I(\omega, \mathbf{k}, \mathbf{k}', \boldsymbol{\epsilon}, \boldsymbol{\epsilon}') \propto \sum_{\mathrm{f}} \left| \sum_{\mathrm{I}} \frac{\langle \mathrm{f}|\hat{H}'_{\mathbf{k}'\boldsymbol{\epsilon}'}|\mathrm{I}\rangle\langle \mathrm{I}|\hat{H}'_{\mathbf{k}\boldsymbol{\epsilon}}|\mathrm{g}\rangle}{E_\mathrm{g} - E_\mathrm{I}} \right|^2 \times \delta(E_\mathrm{f} - E_\mathrm{g} - \hbar\omega), \quad (1)$$

where the δ function enforces energy conservation and the RIXS perturbation operator in the dipolar approximation is given by the lattice sum $\hat{H}'_{\mathbf{k}\boldsymbol{\epsilon}} = \sum_{\mathbf{R}} \hat{\boldsymbol{\alpha}}\boldsymbol{\epsilon} \exp(-i\mathbf{kR})$, where $\hat{\boldsymbol{\alpha}}$ are Dirac matrices. Both the $|g\rangle$ and $|f\rangle$ states are dispersive, so the sum over final states is calculated using the linear tetrahedron method [34].

Detailed expressions for the matrix elements in the electric dipole approximation in the framework of fully relativistic Dirac representation were presented in Ref. [35].

c. Calculation details. The details of the computational method are described in our previous papers [36–39], and here we only mention several aspects. Band structure calculations were performed using the fully relativistic linear muffin-tin orbital (LMTO) method [40,41]. This implementation of the LMTO method uses four-component basis functions constructed by solving the Dirac equation inside an atomic sphere [32]. The exchange-correlation functional of the generalized gradient approximation (GGA) type was used in the version of Perdew, Burke, and Ernzerhof [42]. Brillouin zone integration was performed using the improved tetrahedron method [43]. The basis consisted of Ir s, p, d, and f and Li and O s, p, and d LMTOs.

To take into account electron-electron correlation effects, we used in this work the "relativistic" generalization of the rotationally invariant version of the local spin density approximation (LSDA)+U method [44] which takes into account SO coupling so that the occupation matrix of localized electrons becomes nondiagonal in spin indexes. We use in our calculations the value of $U_{\mathrm{eff}} = 1.5$ eV ($U = 2.15$ eV and $J_H = 0.65$ eV), which gives the best agreement between the calculated and experimental optical spectra in the β-Li_2IrO_3 [30].

We used in our calculations vector $\mathbf{q} = (0, 10, 0)$ real lattice units. Takayama *et al.* [27] show that at a low pressure of 0.9 GPa, the RIXS spectrum at the Ir $L3$ for the single crystal agrees well with that of the polycrystalline sample at ambient pressure. This supports the idea that the d-d excitations show only a small $\mathbf{q}$ dependence in β-Li_2IrO_3.

III. ELECTRONIC STRUCTURE

Figure 1 presents the *ab initio* Ir 5d partial density of states (PDOS) of β-Li_2IrO_3 in an energy range of −2 to 4.7 eV for the ambient pressure $Fddd$ phase, calculated in the fully relativistic Dirac GGA+SO approximation [Fig. 1(a)] and with taking into account Coulomb correlations in the GGA+SO+U approximation [Fig. 1(b)]. Figure 1(c) presents

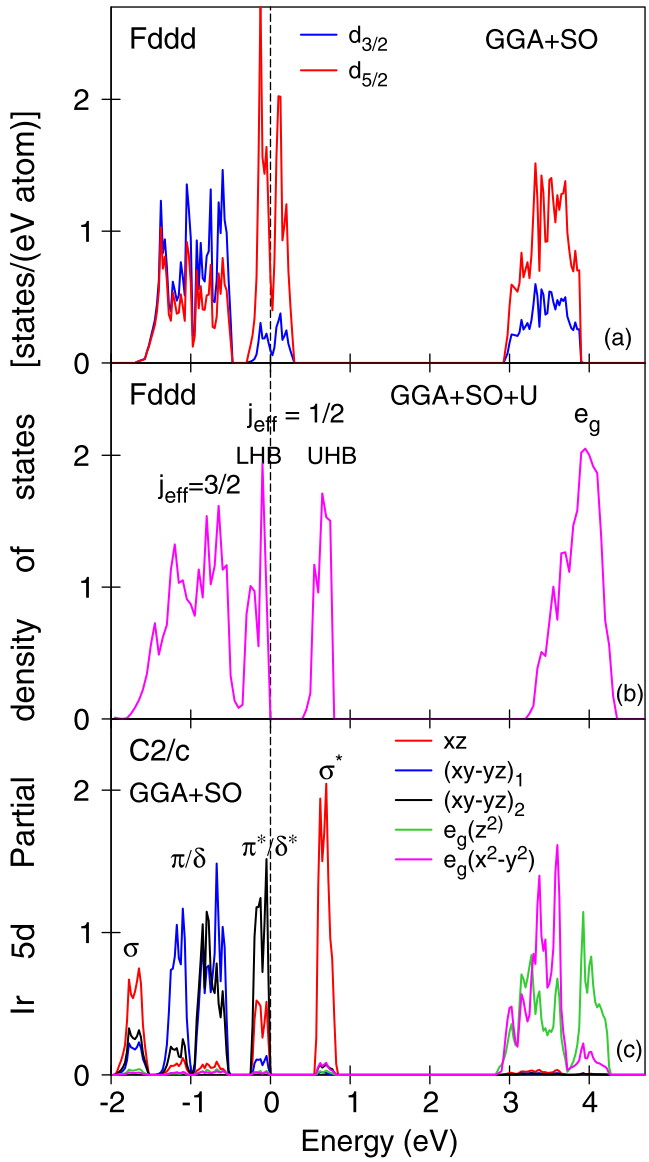

FIG. 1. (a) Ir $5d$ partial density of states [in electrons/(eV atom)] of β-Li_2IrO_3 for the ambient pressure phase ($Fddd$) in the fully relativistic Dirac GGA+SO approximation. (b) The PDOS of β-Li_2IrO_3 for the ambient pressure phase ($Fddd$) in the GGA+SO+U approximation. (c) The PDOSs of the β-Li_2IrO_3 for the high-pressure phase ($C2/c$) in the GGA+SO approach.

the PDOSs of β-Li_2IrO_3 for the high-pressure phase ($C2/c$) in the GGA+SO approach.

The GGA+SO approximation produces a metallic ground state in β-Li_2IrO_3 [Fig. 1(a)], in contradiction with resistivity measurements which claim that β-Li_2IrO_3 is a magnetic Mott insulator. The correct ground state in the orthorhombic structure can be obtained only when the Coulomb interaction and SO coupling are both incorporated. Strong SO coupling splits the six t_{2g} orbitals into two manifolds with $J_{\rm eff} = 3/2$ and $J_{\rm eff} = 1/2$. The $J_{\rm eff} = 3/2$ states are fully filled, and the $J_{\rm eff} = 1/2$ states are half filled. The $J_{\rm eff} = 3/2$ quartet is a mixture of $d_{3/2}$ and $d_{5/2}$ states, while $J_{\rm eff} = 1/2$ is dominated mostly by $d_{5/2}$ states [Fig. 1(a)]. The $J_{\rm eff} = 1/2$ states form a narrow band so that even small $U_{\rm eff} = 1.5$ eV opens Mott gap and splits the $5d_{5/2}$ ($J_{\rm eff} = 1/2$) band into the upper Hubbard band (UHB) above the Fermi level and lower Hubbard band (LHB) below the Fermi level [Fig. 1(b)]. The formation of the $J_{\rm eff}$ bands is a natural consequence of the $J_{\rm eff}$ Hubbard model. The e_g orbitals are almost degenerate at ambient pressure, occupying the 3.4–4.2 eV energy interval.

β-Li_2IrO_3 undergoes a pressure-induced structural phase transition at P_c with symmetry lowering to the monoclinic $C2/c$ structure [27,31]. The phase transition is accompanied by the formation of Ir_2 dimers on the zigzag chains, with an Ir-Ir distance of ∼2.66 Å, even shorter than that of metallic Ir. The strong dimerization stabilizes the bonding molecular-orbital state, leads to the collapse of the magnetism, and opens the energy gap with a concomitant electronic phase transition from a magnetic Mott insulator to a nonmagnetic (NM) noncorrelated band insulator. This phase does not accommodate local $J_{\rm eff} = 1/2$ moments, indicating a delicate balance between magnetism and the intermetallic covalency. This naturally implies the nonessential role of Hubbard U and SO coupling in the high-pressure monoclinic structure. The energy gap is reduced by only 0.5 meV after switching off SO interaction. It is also consistent with the pressure dependence of the branching ratio BR $= I_{L_3}/I_{L_2}$, where $I_{L_{2,3}}$ is the integrated intensity of the isotropic x-ray absorption spectra at the $L_{2,3}$ edges [30,31], and supported by the x-ray magnetic circular dichroism (XMCD) measurements by Takayama *et al.* [15]. They found that the x-ray magnetic circular dichroism is strongly reduced at ∼1.5 GPa and completely suppressed around 2 GPa in β-Li_2IrO_3, indicating a rapid suppression of magnetic-field-induced ferromagnetic moments. These conclusions are also consistent with a neutron and resonant inelastic x-ray scattering study [27] and Raman scattering under pressure [28].

Figure 1(c) presents the *ab initio* PDOSs in β-Li_2IrO_3 for the monoclinic $C2/c$ structure calculated in the fully relativistic Dirac GGA+SO approximation. There are two peaks at −1.7 and 0.7 eV which can be assigned to the σ bonding and antibonding states of Ir_2 dimer molecules. These states possess predominantly d_{xz} character [in the coordinate system $x' = (x + z)/\sqrt{2}$, $y' = (x - z)/\sqrt{2}$, $z' = y$, with the d_{xz} orbital directed along the dimer Y bond]. The large bonding-antibonding splitting stabilizes the d_{xz}-orbital-dominant antibonding σ^* state of t_{2g} holes and makes the system a NM band insulator. SO coupling separates the d_{xy}/d_{yz} bands into two groups, bonding π/δ and antibonding π^*/δ^* states situated at −0.5 to −1.4 and 0 to −0.3 eV, respectively. These orbitals contribute to the subbands between the σ bonding and antibonding subbands due to stronger hybridization between the nearest-neighbor Ir atoms than that of d_{xz} orbitals. An energy gap is formed between the occupied antibonding π^*/δ^* and the empty antibonding σ^* subbands.

Comparing Figs. 1(b) and 1(c), we can see that the energy position of the antibonding σ^* peak in the NM high-pressure $C2/c$ phase coincides with the position of the corresponding UHB $J_{\rm eff} = 1/2$ states in the magnetic Mott insulator at ambient pressure.

Due to the strong distortion of IrO_6 octahedra in the $C2/c$ high-pressure phase the e_g orbitals, which are almost degenerate at ambient pressure, split into z^2 and x^2-y^2 states and become broader, occupying the 3–4.5 eV energy interval.

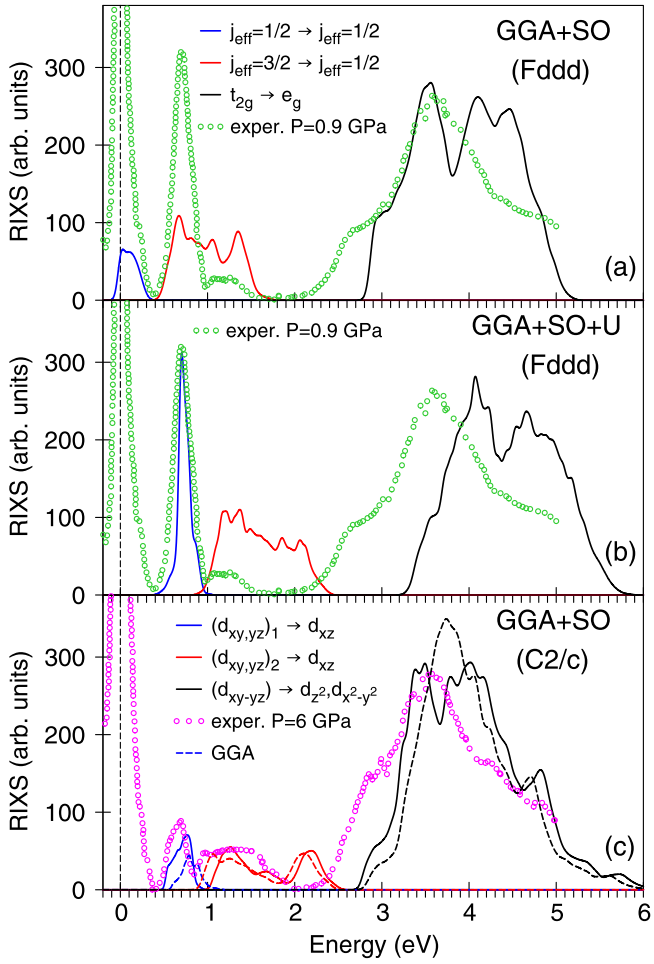

FIG. 2. (a) The experimental RIXS spectra at the Ir L_3 edge for β-Li_2IrO_3 for ambient pressure at room temperature [27] (open green circles) compared with the theoretically calculated spectra in the GGA+SO approximation. (b) The experimental RIXS spectra at the Ir L_3 edge for β-Li_2IrO_3 for ambient pressure [27] (open green circles) compared with the theoretically calculated spectra in the GGA+SO+U approach (solid curves). (c) The experimental RIXS spectra at the Ir L_3 edge for β-Li_2IrO_3 for the high-pressure phase ($C2/c$) above P_c [27] (open magenta circles) compared with the theoretically calculated spectra in the GGA+SO (solid lines) and GGA (dashed lines) approximations.

IV. Ir L_3 RIXS SPECTRUM

Figure 2 presents the experimentally measured RIXS spectrum at the Ir L_3 edge for β-Li_2IrO_3 for ambient pressure [27] (green open circles) compared with the theoretically calculated ones in the GGA+SO [Fig. 2(a)] and GGA+SO+U [Fig. 2(b)] approximations for the $Fddd$ phase. Figure 2(c) shows the experimental RIXS spectrum for the high-pressure phase ($C2/c$) above P_c [27] (open magenta circles) compared with the theoretically calculated spectra in the GGA+SO approximation.

The experimental RIXS spectrum at the Ir L_3 edge for ambient pressure in addition to the elastic scattering peak at 0 eV possesses a sharp narrow peak at around 0.7 eV, followed by a broad structure between 1 and 2 eV and a broad peak centered at around 3.5 eV. The latter represents the excitations from Ir $5d$ t_{2g} to e_g manifolds. The peak at ~0.7 eV can be assigned to the local excitation between the filled $J_{\text{eff}} = 1/2$ and empty $J_{\text{eff}} = 1/2$ states. The fine structure at 1 to 2 eV is derived by the excitation between the filled $J_{\text{eff}} = 3/2$ and empty $J_{\text{eff}} = 1/2$ states.

The GGA+SO approximation fails to reproduce a sharp narrow peak at around 0.7 eV. The corresponding peak is situated at 0.1 eV [blue curve in Fig. 2(a)] and has a much lower intensity in comparison with the experimentally observed peak at 0.7 eV. On the other hand, the theory correctly reproduces the energy position of the wide peak at 3.5 eV responsible for the $t_{2g} \rightarrow e_g$ transitions [black curve in Fig. 2(a)]. In contrast, the GGA+SO+U approach well describes the shape and intensity of the LHB $J_{\text{eff}} = 1/2 \rightarrow$ UHB $J_{\text{eff}} = 1/2$ peak at 0.7 eV. We calculated the RIXS spectra for the ferromagnetic and antiferromagnetic ordering along the c direction and in the ab plane for the $Fddd$ phase and found that the type of magnetic ordering weakly influences the shape and intensity of the major fine structures of the Ir L_3 RIXS spectrum.

Figure 2(c) presents the experimental RIXS spectra at the Ir L_3 edge for β-Li_2IrO_3 for high-pressure $C2/c$ [27] in comparison with the theoretically calculated spectrum in the GGA+SO (solid lines) and GGA (dashed lines) approximations. Although SO coupling has a minor influence on the value of the energy gap in high-pressure $C2/c$, it influences the shape and intensity of the RIXS spectrum.

Comparing Figs. 2(b) and 2(c), we can conclude that although there is reasonable agreement between the theoretically calculated and experimental RIXS spectra for the high-pressure $C2/c$ structure, the GGA+SO+U approach provides an unsatisfactory description of the RIXS spectrum in the ambient pressure $Fddd$ phase. The calculations overestimate the intensity of the fine structure in the 1 to 1.5 eV energy region and shift the Ir $t_{2g} \rightarrow e_g$ peak towards higher energy. We should mention, however, that the energy position of e_g states is very sensitive to sample preparation and sample quality. For example, the energy positions of the Ir $t_{2g} \rightarrow e_g$ peak in the iridate $Eu_2Ir_2O_7$ in Hozoi *et al.*'s [45] and Clancy *et al.*'s [46] measurements differ from each other by approximately 0.5 eV. On the other hand, the GGA+SO+U approach produces excellent agreement in the energy position and intensity of the prominent peak at 0.7 eV (which is our major concern).

We should mention that the GGA+U method, which combines the GGA with a basically static, i.e., Hartree-Fock-like, mean-field approximation for a multiband Anderson lattice model, does not contain true many-body physics. This method is too simple to capture all the peculiarities of the electronic correlations in β-Li_2IrO_3. Applications of new many-body approaches such as dynamical mean-field approximation (GGA+DMFT) and multiplet structure calculations to the calculations of the electronic structure and RIXS spectra of β-Li_2IrO_3 are highly desirable.

Both the ambient pressure ($Fddd$) and high-pressure ($C2/c$) phases possess an empty peak in proximity to the Fermi level at around 0.7 eV (Fig. 1); therefore, one would expect similar RIXS spectra in the low-energy range below 1 eV. However, RIXS measurements show the drastic reconstruction of the electronic structure associated with the Ir

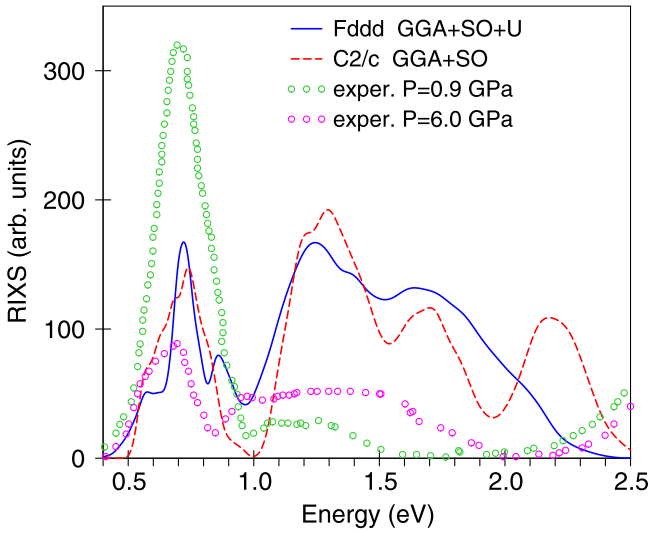

FIG. 3. Comparison of RIXS spectra for the ambient (green circles) and high pressure above P_c (magenta circles) phases [27] with the constant matrix elements (JDOS) calculated for the ambient pressure phase ($Fddd$) in the GGA+SO+U approximation (solid blue curve) and for the high-pressure phase ($C2/c$) in the GGA+SO approach (dashed red curve).

dimerization [27]. The 0.7 eV peak is suppressed strongly in the high-pressure dimerized phase above 4 GPa.

The RIXS spectrum is a convolution of the densities of the occupied and empty valence states [the so-called joint density of states (JDOS)], weighted by appropriate matrix elements. Figure 3 presents a comparison of the experimentally measured RIXS spectra for the ambient and high-pressure phases [27] with the JDOS calculated for the ambient pressure phase ($Fddd$) in the GGA+SO+U approximation (the solid blue curve) and for the high-pressure phase ($C2/c$) in the GGA+SO approach (the dashed red curve). We see that without taking into account the corresponding matrix elements the theoretically calculated prominent peak at 0.7 eV has similar intensities for both phases and significantly differs from the experimentally measured ones. Therefore, the reason for strong suppression of this peak in the high-pressure phase is the significantly different matrix elements in these two phases.

There are two reasons why the matrix elements can be strongly altered in the phase transition at P_c. First, the prominent peak at 0.7 eV above the Fermi level is created by different orbitals (t_{2g} states in the $Fddd$ phase and almost pure d_{xz} orbitals in the high-pressure $C2/c$ phase). Yang *at al.* [47] showed that angular matrix elements for dipole-allowed transitions in x-ray absorption at the L_3 edge strongly depend on the type of orbitals involved in the transitions. Second, the matrix elements can be strongly modified due to different ground states of the phases: a magnetic strongly correlated Mott insulator at ambient pressure and a NM noncorrelated band insulator at P_c with vanished Hubbard U.

We examine the dependence of the RIXS spectra on the Hubbard U at the Ir site, calculating the spectra for $U =$ 2.15, 1.9, 1.65, 1.4, 1.15, 0.9, and 0.65 eV. It corresponds to $U_{\text{eff}} = 1.5$, 1.25, 1.0, 0.75, 0.5, 0.25 eV, and 0 eV. The results of these calculations for the RIXS spectra dependence

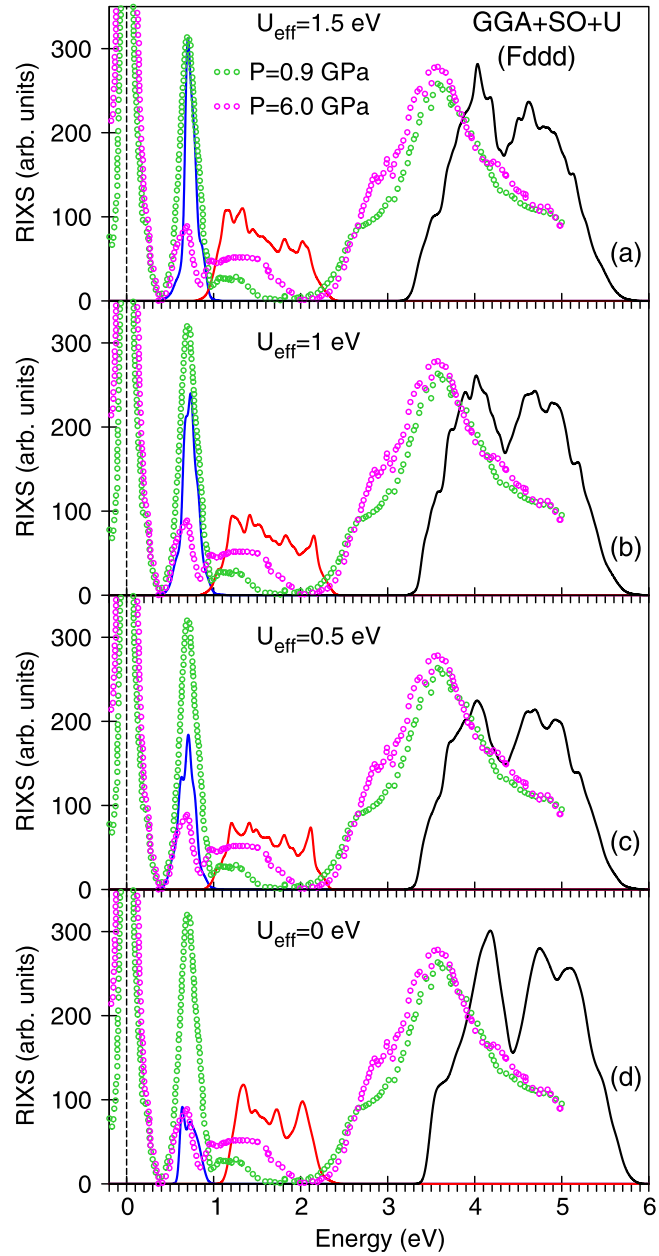

FIG. 4. The experimental RIXS spectra at the Ir L_3 edge for β-Li_2IrO_3 for the ambient pressure ($Fddd$; open green circles) and high-pressure (open magenta circles; $C2/c$) phases above P_c [27] compared with the theoretically calculated spectra in the GGA+SO+U approximation for different values of U_{eff} at the Ir site.

on U_{eff} are shown in Fig. 4. The reduction of U_{eff} leads to a gradual reduction of the peak intensity of the prominent peak at 0.7 eV. For $U_{\text{eff}} = 0$ eV this peak reduces to the value observed in the high-pressure phase. We found that the energy gap is also reduced by 0.102, 0.202, and 0.301 eV for $U_{\text{eff}} =$ 1.25, 1.0, and 0.75 eV, respectively. The gap is closed for $U_{\text{eff}} = 0.5$ eV. As a result, the prominent peak situated at 0.7 eV shifts towards lower energy with the decreasing of the U_{eff} parameter. To show more clearly how the peak intensity at 0.7 eV depends on U_{eff} we keep this peak artificially at 0.7 eV above the Fermi level in Fig. 4.

We can conclude that the drastic reconstruction of the RIXS spectrum associated with the structural $Fddd \rightarrow C2/c$ phase transition at P_c is related to the Coulomb correlations disappearing in the high-pressure $C2/c$ phase.

V. CONCLUSIONS

The electronic structure and RIXS spectra of the hyper-honeycomb iridate β-Li_2IrO_3 were investigated theoretically within the density-functional theory GGA approach in the framework of the fully relativistic spin-polarized Dirac LMTO band structure method, taking into account Coulomb electron-electron correlations.

The GGA+SO approximation produces a metallic ground state in β-Li_2IrO_3, in contradiction to resistivity measurements which claim that β-Li_2IrO_3 is a magnetic Mott insulator. The correct ground state in the orthorhombic structure can be obtained only when the Coulomb interaction and SO coupling are both incorporated. The Coulomb repulsion U_{eff} splits the half-filled $J_{\text{eff}} = 1/2$ band into an empty UHB band with pure $d_{5/2}$ character and occupied LHB.

β-Li_2IrO_3 undergoes a pressure-induced structural phase transition at P_c with symmetry lowering to the monoclinic $C2/c$ structure. The phase transition is accompanied by the formation of Ir_2 dimers on the zigzag chains. The strong dimerization stabilizes the bonding molecular-orbital state, leads to the collapse of the magnetism, and opens the energy gap with a concomitant electronic phase transition from the magnetic Mott insulator to nonmagnetic noncorrelated band insulator. This phase does not accommodate local $J_{\text{eff}} = 1/2$ moments, indicating a delicate balance between magnetism and the intermetallic covalency. This naturally implies the nonessential role of Hubbard U and SO coupling in the high-pressure monoclinic structure.

Both the ambient pressure ($Fddd$) and high-pressure ($C2/c$) phases possess an empty peak in proximity to the Fermi level at around 0.7 eV; therefore, one would expect similar RIXS spectra in the low-energy range below 1 eV. However, RIXS measurements show the drastic reconstruction of the electronic structure associated with the Ir dimerization. The reconstruction of the RIXS spectral peak at 0.7 eV associated with the structural $Fddd \rightarrow C2/c$ phase transition at P_c can be related to the disappearing of the Coulomb correlations.

Although there is reasonable agreement between the theoretically calculated and experimental RIXS spectra for the high-pressure $C2/c$ structure the GGA+SO+U approach provides an unsatisfactory description of the RIXS spectrum in the ambient pressure $Fddd$ phase. The calculations shift the Ir $t_{2g} \rightarrow e_g$ peak towards higher energy and overestimate the intensity of the fine structure in the 1 to 1.5 eV energy region. However, it produces excellent agreement in the energy position and intensity of the prominent peak at 0.7 eV.

We should mention that the GGA+U method, which combines the GGA with a basically static, i.e., Hartree-Fock-like, mean-field approximation for a multiband Anderson lattice model does not contain true many-body physics. This method is too simple to capture all the peculiarities of the electronic correlations in β-Li_2IrO_3. Applications of new many-body approaches such as GGA+DMFT and multiplet structure calculations to the electronic structure and RIXS spectra of β-Li_2IrO_3 are highly desirable.

ACKNOWLEDGMENTS

We are thankful to Dr. A. Yaresko from Max-Planck-Institute FKF in Stuttgart for very long and helpful discussions. V.N.A. gratefully acknowledges the hospitality at the University of Bialystok during his stay there. D.A.K. gratefully acknowledges the hospitality at the Max-Planck-Institute FKF during his stay in Stuttgart. The studies were supported by the National Academy of Sciences of Ukraine within the budget program KPKBK 6541230-3A, "Support for the development of priority areas of scientific research."

[1] G. Jackeli and G. Khaliullin, Phys. Rev. Lett. **102**, 017205 (2009).
[2] W. Witczak-Krempa, G. Chen, Y. B. Kim, and L. Balents, Annu. Rev. Condens. Matter Phys. **5**, 57 (2014).
[3] I. Kimchi, J. G. Analytis, and A. Vishwanath, Phys. Rev. B **90**, 205126 (2014).
[4] A. Kitaev, Ann. Phys. (NY) **321**, 2 (2006).
[5] S. M. Albrecht, A. P. Higginbotham, M. Madsen, F. Kuemmeth, T. S. Jespersen, J. Nygrd, P. Krogstrup, and C. M. Marcus, Nature (London) **531**, 206 (2016).
[6] S. M. Winter, A. A. Tsirlin, M. Daghofer, J. van den Brink, Y. Singh, P. Gegenwart, and R. Valenti, J. Phys.: Condens. Matter **29**, 493002 (2017).
[7] R. Schaffer, E. K.-H. Lee, B.-J. Yang, and Y. B. Kim, Rep. Prog. Phys. **79**, 094504 (2016).
[8] F. Ye, S. Chi, H. Cao, B. C. Chakoumakos, J. A. Fernandez-Baca, R. Custelcean, T. F. Qi, O. B. Korneta, and G. Cao, Phys. Rev. B **85**, 180403 (2012).
[9] A. Shitade, H. Katsura, J. Kunes, X.-L. Qi, S.-C. Zhang, and N. Nagaosa, Phys. Rev. Lett. **102**, 256403 (2009).
[10] M. Z. Hasan and C. L. Kane, Rev. Mod. Phys. **82**, 3045 (2010).
[11] J. Chaloupka, G. Jackeli, and G. Khaliullin, Phys. Rev. Lett. **110**, 097204 (2013).
[12] G. Cao, T. F. Qi, L. Li, J. Terzic, V. S. Cao, S. J. Yuan, M. Tovar, G. Murthy, and R. K. Kaul, Phys. Rev. B **88**, 220414 (2013).
[13] A. Biffin, R. D. Johnson, S. Choi, F. Freund, S. Manni, A. Bombardi, P. Manuel, P. Gegenwart, and R. Coldea, Phys. Rev. B **90**, 205116 (2014).
[14] J. Knolle, G.-W. Chern, D. L. Kovrizhin, R. Moessner, and N. B. Perkins, Phys. Rev. Lett. **113**, 187201 (2014).
[15] T. Takayama, A. Kato, R. Dinnebier, J. Nuss, H. Kono, L. S. I. Veiga, G. Fabbris, D. Haskel, and H. Takagi, Phys. Rev. Lett. **114**, 077202 (2015).
[16] R. Schaffer, E. K.-H. Lee, Y.-M. Lu, and Y. B. Kim, Phys. Rev. Lett. **114**, 116803 (2015).
[17] A. Glamazda, P. Lemmens, S. H. Do, Y. S. Choi, and K. Y. Choi, Nat. Commun. **7**, 12286 (2016).
[18] B. J. Kim, H. Jin, S. J. Moon, J.-Y. Kim, B.-G. Park, C. S. Leem, J. Yu, T. W. Noh, C. Kim, S.-J. Oh, J.-H. Park,

V. Durairaj, G. Cao, and E. Rotenberg, Phys. Rev. Lett. **101**, 076402 (2008).
[19] H.-S. Kim, Y. B. Kim, and H.-Y. Kee, Phys. Rev. B **94**, 245127 (2016).
[20] E. K.-H. Lee and Y. B. Kim, Phys. Rev. B **91**, 064407 (2015).
[21] I. Kimchi, R. Coldea, and A. Vishwanath, Phys. Rev. B **91**, 245134 (2015).
[22] V. M. Katukuri, R. Yadav, L. Hozoi, S. Nishimoto, and J. van den Brink, Sci. Rep. **6**, 29585 (2016).
[23] A. Ruiz, A. Frano, N. P. Breznay, I. Kimchi, T. Helm, I. Oswald, J. Y. Chan, R. Birgeneau, Z. Islam, and J. G. Analytis, Nat. Commun. **8**, 961 (2017).
[24] S. Ducatman, I. Rousochatzakis, and N. B. Perkins, Phys. Rev. B **97**, 125125 (2018).
[25] M. Majumder, R. S. Manna, G. Simutis, J. C. Orain, T. Dey, F. Freund, A. Jesche, R. Khasanov, P. K. Biswas, E. Bykova, N. Dubrovinskaia, L. S. Dubrovinsky, R. Yadav, L. Hozoi, S. Nishimoto, A. A. Tsirlin, and P. Gegenwart, Phys. Rev. Lett. **120**, 237202 (2018).
[26] V. Hermann, M. Altmeyer, J. Ebad-Allah, F. Freund, A. Jesche, A. A. Tsirlin, M. Hanfland, P. Gegenwart, I. I. Mazin, D. I. Khomskii, R. Valentí, and C. A. Kuntscher, Phys. Rev. B **97**, 020104(R) (2018).
[27] T. Takayama, A. Krajewska, A. S. Gibbs, A. N. Yaresko, H. Ishii, H. Yamaoka, K. Ishii, N. Hiraoka, N. P. Funnell, C. L. Bull, and H. Takagi, Phys. Rev. B **99**, 125127 (2019).
[28] S. Choi, H.-S. Kim, H.-H. Kim, A. Krajewska, G. Kim, M. Minola, T. Takayama, H. Takagi, K. Haule, D. Vanderbilt, and B. Keimer, Phys. Rev. B **101**, 054102 (2020).
[29] L. J. P. Ament, M. van Veenendaal, T. P. Devereaux, J. P. Hill, and J. van den Brink, Rev. Mod. Phys. **83**, 705 (2011).
[30] V. N. Antonov, S. Uba, and L. Uba, Phys. Rev. B **98**, 245113 (2018).
[31] L. S. I. Veiga, M. Etter, K. Glazyrin, F. Sun, J. C. A. Escanhoela, Jr., G. Fabbris, J. R. L. Mardegan, P. S. Malavi, Y. Deng, P. P. Stavropoulos, H.-Y. Kee, W. G. Yang, M. van Veenendaal, J. S. Schilling, T. Takayama, H. Takagi, and D. Haskel, Phys. Rev. B **96**, 140402(R) (2017).
[32] V. V. Nemoshkalenko, A. E. Krasovskii, V. N. Antonov, V. N. Antonov, U. Fleck, H. Wonn, and P. Ziesche, Phys. Status Solidi B **120**, 283 (1983).
[33] E. Arola, P. Strange, and B. L. Gyorffy, Phys. Rev. B **55**, 472 (1997).
[34] G. Lehmann and M. Taut, Phys. Status Solidi B **54**, 469 (1972).
[35] D. A. Kukusta and A. N. Yaresko (unpublished).
[36] V. N. Antonov, O. Jepsen, A. N. Yaresko, and A. P. Shpak, J. Appl. Phys. **100**, 043711 (2006).
[37] V. N. Antonov, B. N. Harmon, A. N. Yaresko, and A. P. Shpak, Phys. Rev. B **75**, 184422 (2007).
[38] V. N. Antonov, A. N. Yaresko, and O. Jepsen, Phys. Rev. B **81**, 075209 (2010).
[39] V. N. Antonov, L. V. Bekenov, and D. A. Kukusta, Phys. Rev. B **102**, 195134 (2020).
[40] O. K. Andersen, Phys. Rev. B **12**, 3060 (1975).
[41] A. Y. Perlov, A. N. Yaresko, and V. N. Antonov (unpublished).
[42] J. P. Perdew, K. Burke, and M. Ernzerhof, Phys. Rev. Lett. **77**, 3865 (1996).
[43] P. E. Blöchl, O. Jepsen, and O. K. Andersen, Phys. Rev. B **49**, 16223 (1994).
[44] A. N. Yaresko, V. N. Antonov, and P. Fulde, Phys. Rev. B **67**, 155103 (2003).
[45] L. Hozoi, H. Gretarsson, J. P. Clancy, B.-G. Jeon, B. Lee, K. H. Kim, V. Yushankhai, P. Fulde, D. Casa, T. Gog, J. Kim, A. H. Said, M. H. Upton, Y.-J. Kim, and J. van den Brink, Phys. Rev. B **89**, 115111 (2014).
[46] J. P. Clancy, H. Gretarsson, E. K. H. Lee, D. Tian, J. Kim, M. H. Upton, D. Casa, T. Gog, Z. Islam, B.-G. Jeon, K. H. Kim, S. Desgreniers, Y. B. Kim, S. J. Julian, and Y.-J. Kim, Phys. Rev. B **94**, 024408 (2016).
[47] X. Yang, A. N. Yaresko, V. N. Antonov, and O. K. Andersen, arXiv:0911.4349.